Long exposure point spread function reconstruction for laser guide star multi conjugate adaptive optics

L.Gilles[1], B.Ellerbroek[1], L.Wang[1], C.Correia[2] and J.P.Véran[2]

[1]Thirty Meter Telescope Observatory Corp., 1200 E. California Blvd, MC 102-8, Pasadena, CA 91125, USA
E-mail: lgilles@caltech.edu, Phone: 1 626 395 1622, Fax: 1 626 395 8909
[2]NRC Herzberg Institute of Astrophysics, 5171 W. Saanich Road, Victoria, BC, V9E 2E7, Canada

Abstract. This paper discusses a simulation-based approach for long exposure point spread function reconstruction (PSFR) for laser guide star (LGS) multi conjugate adaptive optics (MCAO). The approach is based on (i) processing the on-axis high-order LGS wavefront sensor (WFS) second-order statistics to compute via simulation a tip/tilt removed (TTR) structure function (SF) for the science target at infinite range, and (ii) processing similarly the multiple low-order natural guide star (NGS) WFSs controlling tip/tilt (TT) and tilt anisoplanatism (TA) over an extended field of view (FoV) to compute via simulation a tip/tilt (TT) SF for the science target, and (iii) finally summing both SFs. Several options for computing the SFs are discussed. Such an approach to PSFR is general enough that is fully applicable to any type of tomographic and non-tromographic AO system, employing either laser or exclusively natural guide stars.

1. Introduction

Point spread function (PSF) knowledge is critical for any existing or proposed adaptive optics (AO) astronomical science program aiming at obtaining high angular resolution information. Examples of such programs include photometry and astrometry in crowded and sparse stellar fields, detection and characterization of exoplanets, determining precision orbits at the Galactic Center (GC) to test general relativity and black hole growth models, dynamics of early galaxies, and gravitational lensing [1,2,3,4,5].

AO systems on future extremely large telescopes (ELTs) are required to meet tight photometric and astrometric budgets. For instance, the Narrow Field Infrared Adaptive Optics System (NFIRAOS) under design for the Thirty Meter Telescope (TMT) is required to provide 2% differential photometry over a 30" field of view (FoV) for a 10 min integration in J band, and 50 mircroarcsec root-mean-square (RMS) time dependent differential astrometry over the same FoV for a 100 sec integration in H band [6,7]. Flowing down point spread function reconstruction (PSFR) accuracy requirements from these top-level photometric and astrometric requirements is therefore an important question.

Véran pioneered AO PSFR in 1997 by developing a practical method to reconstruct the long exposure PSF of a bright natural guide star (NGS) from wavefront sensor (WFS) second-order statistics [8]. Fusco in 2000 [9], and later Britton in 2005 [10], extended PSFR to capture a key missing component: angular anisoplanatism, providing the astronomical AO community a complete PSFR tool for classical NGS single-conjugate AO (SCAO) observations. 4% Strehl ratio (SR) errors in K-band are reported on the Palomar AO system (order 16 x 16) at the 5 m Hale Telescope [10] for observations of a bright star separated by 21" from its companient star. Measurements of the turbulence profile from a multi-aperture scintillation sensor (MASS) and a differential image motion monitor (DIMM) provided the necessary input for the off-axis PSFR in these experiments. Recently, Jollissaint reported 5% K-band SR error at the 10 m Keck Telescope for bright NGS AO observations [11]. Jolissaint stresses two critical aspects of PSFR: the estimation of (i) the static/quasi-static optical aberrations (common and non-common path), and (ii) the atmospheric turbulence profile. Flicker, in 2008, pushed the theory further to include focal anisoplanatism (i.e. the cone effect), opening the door to PSFR for LGS SCAO [12].

PSFR for LGS multi conjugate adaptive optics (MCAO) on ELTs faces multiple additional challenges. The effects of angular anisoplanatism are very different for LGS MCAO. The PSF is much more uniform across an extended FoV characterized by the generalized isoplanatic angle [13], and the SR of point sources at infinity is actually larger than that of point sources at finite-range, making an analytical derivation of the anisoplanatism filter function difficult. Another important difference is the nature of the telemetry data. Multiple high-order (HO) LGS WFSs are required in LGS MCAO to perform HO atmospheric tomography, and similarly, multiple low-order (LO) NGS WFSs are required to correct tilt anisoplanatism (TA) (LO tomographic modes invisible by the LGS WFSs) across the FoV [14].

For these reasons, we opted to base our approach on a high-speed, high-fidelity, end-to-end Monte Carlo numerical simulation tool, fed by the necessary real-time computer (RTC) *system telemetry data*, including the turbulence profile estimated in real-time during LGS tomography from a pair of LGS WFSs [15], WFS signal levels and control loop parameters (WFS subaperture centroiding algorithms, tomography reconstruction

algorithms, servo parameters, etc.). With the advent of more mature graphics processing unit (GPU) technology, it is now possible to run high-fidelity end-to-end Monte Carlo simulations at the real-time speed of current 10 m class astronomical AO telescopes, and similar speed ratios are within reach for currently designed ELTs. For instance, a full fidelity simulation of NFIRAOS in the multi-threaded adaptive optics simulator (MAOS) running on a pair of GTX580 GPUs is currently only about two orders of magnitude slower than the real-time speed (100 ms/frame, system running at 800 Hz) [16]. It is thus conceivable to feed such an AO simulator with data gathered from the telescope, AO system and science instrument, in an attempt to closely mimic in simulation the actual system behavior. This paper discusses how such a powerful tool could be used to perform PSFR for LGS MCAO.

The paper is organized as follows. Section 1 provides a top-level description of our approach, which is then further detailed in subsections 3, 2.2 and 2.3. Results will be reported in a forthcoming publication.

2. Top-level description of the approach

A block diagram of the approach is shown in Figure 1. The long exposure optical transfer function (OTF) (Fourier transformed PSF) at each science field point is modeled as the product of the TTR OTF and a TT filter. The error introduced by this TT decoupling assumption has been characterized for NFIRAOS in terms of Strehl ratio (SR) and enclosed energy (EE) in a separate publication [17]. The error was found to be below the percent level in J-band over a 17''x17'' FoV, depending on the level of residual TT and TA wavefront error (median TT/TA NFIRAOS wavefront error is about $\lambda/20$ RMS in J-band). A high-speed, high-fidelity, end-to-end Monte Carlo numerical simulation tool, fed by critical real-time computer (RTC) system telemetry data provides an estimate of the TTR and TT OTF components. Since the residual phase may in general have a non-zero temporal mean on account of opto-mechanical static/quasi-static biases and a finite exposure time, the reconstructed OTF will in general be complex-valued. This means that the reconstructed PSF will in general be non-symmetric. The reconstructed OTF is thus modeled as the following 2-term product:

$$\widehat{OTF}(u) = \widehat{K}_{TT}(u)\widehat{OTF}_{TTR}(u), \tag{2.1}$$

where the TT transfer function is given by:

$$\widehat{K}_{TT}(u) = e^{ik<\hat{\Delta}_{TT}(\lambda u)>} e^{-k^2 \hat{D}_{TT}(\lambda u)/2}, \tag{2.2}$$

and the TTR OTF by:

$$\widehat{OTF}_{TTR}(u) = \int d^2x A(x)A(x+\lambda u) e^{ik<\hat{\Delta}_{TTR}(x,x+\lambda u)>} e^{-k^2 \hat{D}_{TTR}(x,x+\lambda u)/2}, \tag{2.3}$$

where we used the fact for a normally distributed disturbance $< e^{i\phi} >= e^{i<\phi>} e^{-\sigma_\phi^2/2}$. In all these expressions, u denotes the focal plane angular spatial frequency variable, $k = 2\pi/\lambda$ the angular wavenumber, λ the wavelength, $A(x)$ the real-valued unit area pupil function, $\hat{\Delta}(x,x') = \hat{\phi}(x) - \hat{\phi}(x')$ the wavefront difference function (DF), which is related to the structure function (SF) as follows:

$$\hat{D}(x,x') = \left\langle \hat{\Delta}^2(x,x') \right\rangle - \left\langle \hat{\Delta}(x,x') \right\rangle^2. \tag{2.4}$$

The mean TT DF is given by the following expression:

$$\left\langle \hat{\Delta}_{TT}(\lambda u) \right\rangle = 4(\delta\theta)(< \hat{c}_2 > u_x + < \hat{c}_3 > u_y), \tag{2.5}$$

where $\delta\theta = \lambda / D$, and c_2, c_3 are the Zernike tip and tilt coefficients. Substituting (2.5) into (2.4) yields the following expression for the residual TT SF:

$$\hat{D}_{TT}(\lambda u) = 16(\delta\theta)^2 (\hat{\rho}_{22} u_x^2 + \hat{\rho}_{33} u_y^2 + 2\hat{\rho}_{23} u_x u_y), \tag{2.6}$$

where $\hat{\rho}_{kl} =< [\hat{c}_k - < \hat{c}_k >][\hat{c}_l - < \hat{c}_l >] >$ denotes the estimated cross-covariance between Zernike modes $2 \le k, l \le 3$. Note that it is not necessary to make any spatial stationarity or pupil averaging assumption on the SF. $\hat{D}(x,x')$ is expected to be a function of both x and x', and, as pointed out by Flicker [12], can be computed from the 4D covariance function (CF) $\hat{C}(x,x') = \left\langle [\hat{\phi}(x) - < \hat{\phi}(x) >][\hat{\phi}(x') - < \hat{\phi}(x') >] \right\rangle$ as follows:

$$\hat{D}(x,x') = \hat{C}(x,x) + \hat{C}(x',x') - 2\hat{C}(x,x'). \tag{2.7}$$

A suitable method for reconstructing the TT and TTR bias terms $\left\langle \hat{\Delta}_{TT} \right\rangle, \left\langle \hat{\Delta}_{TTR} \right\rangle$ (which will in general be field dependent) is still under investigation. System telemetry includes the turbulence profile estimated in real-time during LGS tomography from a pair of LGS WFSs [15], WFS signal levels and several control loop parameters like WFS subaperture centroiding algorithms, tomography reconstruction algorithm, and servo parameters.

The total SF reconstruction error can be expressed in terms of TTR and TT SF reconstruction errors as follows:

$$\epsilon = \rho_{TTR}\delta_{TTR} + \rho_{TT}\delta_{TT}, \tag{2.8}$$

where $\epsilon = \hat{D}/D$, $\rho_{TTR} = \hat{D}_{TTR}/D_{TTR}$, $\delta_{TTR} = D_{TTR}/D$, and similarly for the TT component. For the case of perfect TTR/TT SF reconstruction, $\rho_{TTR} = \rho_{TT} = 1$, in which case the total SF error is equal to the TT decoupling error.

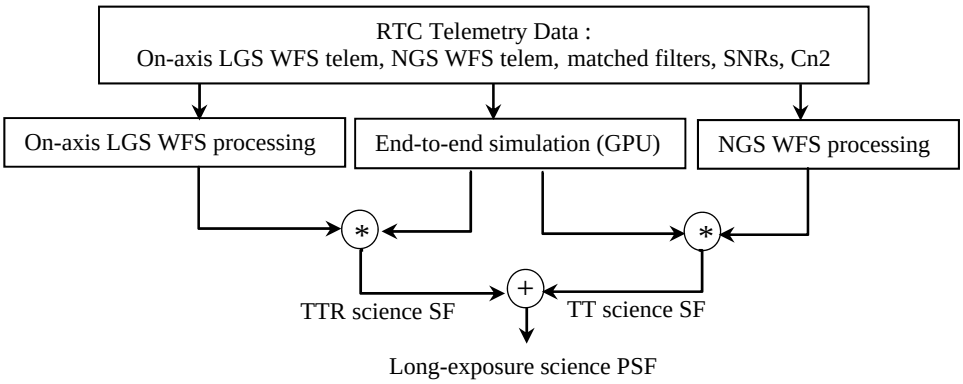

Figure 1 Block diagram illustrating the simulation-based PSFR approach. For each science direction, the SF is decomposed into the sum of a TTR and a TT SF, each reconstructed from a blend of system and simulation data. The TTR SF is reconstructed by processing the closed loop measurement covariance matrix of the high-order on-axis LGS WFS (which points to the science target); the TT SF is reconstructed by processing the closed loop measurement covariance matrix of the multiple low-order NGS WFSs.

In order to reconstruct the TTR and TT components of the SF, we propose to properly filter the corresponding simulation SFs by a *system-to-simulation SF ratio*, i.e.

$$\hat{D}_{TTR} = W_{TTR} D_{TTR}^{sim}, \quad \hat{D}_{TT} = W_{TT} D_{TT}^{sim}, \tag{2.9}$$

where W_{TTR}, W_{TT} are the *SF filters*. Such a filtering procedure provides robustness against any Fried paramater detuning since both science and LGS SFs scale similarly in this parameter. More details on the SF filters are given in the next subsections.

2.1. TTR SF filter

The TTR SF filter is given by the system-to-simulation SF ratio of the *on-axis LGS SFs*, i.e. SFs computed for an on-axis (i.e. at the center of the science FoV) point source at the range of the on-axis LGS. LGS SFs are TTR since TT is poorly measured by LGS WFSs [18]. We consider two types of TTR filters : *unbalanced* and *balanced*, that differ only in their definition of the denominator SF. Both filters use as numerator the reconstructed system LGS SF, computed following Véran's approach [8], i.e. a sum of 4 terms corresponding to (i) telemetry, (ii) noise, (iii) aliasing and (iv) fitting contributions:

$$\hat{D}_{LGS} = \hat{D}_{LGS,telem} - \hat{D}_{LGS,nse} + \alpha \hat{D}_{LGS,alias} + \hat{D}_{fit}, \tag{2.10}$$

where $-1 \le \alpha \le 1$ is an aliasing tuning parameter (possibly retrieved from a precomputed lookup table). Reconstruction of the on-axis LGS SF using (2.10) is presented in a separate paper [19]. The telemetry

contribution is obtained from the system RTC on-axis LGS WFS measurement closed loop covariance matrix, while the noise contribution is obtained from the system RTC on-axis LGS WFS signal level, signal-to-noise ratio, detector model and centroiding algorithm used during the science exposure. The aliasing and fitting contributions (both scaling as the negative 5/3 power of the Fried parameter) are precomputed quantities that can be evaluated either semi-analytically or by an offline simulation [12]. The unbalanced filter uses the simulation LGS SF (as delivered by the simulation without performing any reconstruction) as denominator, whereas the balanced filter uses the reconstructed simulation LGS SF. Note that for the balanced filter, reconstruction is to be performed with the same number of terms for the system and simulation. These terms can be either all 4 terms or only the telemetry and noise terms (2 terms), since aliasing and fitting is expected to be very similar in both system and simulation. Mathematically, the unbalanced filter is thus expressed as follows :

$$W_{TTR} = \frac{\hat{D}_{LGS}}{D_{LGS}^{sim}}, \tag{2.11}$$

whereas the balanced filter takes the form :

$$W_{TTR} = \frac{\hat{D}_{LGS}}{\hat{D}_{LGS}^{sim}}. \tag{2.12}$$

Note the hat appearing in the denominator of (2.12). The reconstruction error for the unbalanced filter is given by the following expression :

$$\rho_{TTR} = \rho_{LGS} \frac{A}{A^{sim}}, \tag{2.13}$$

where $A = D_{LGS} / D_{TTR}$ denotes the system (focal and angular) anisoplanatism SF filter, and similarly $A^{sim} = D_{LGS}^{sim} / D_{TTR}^{sim}$. Two limits are of interest. In the *matched simulation limit* (i.e. the simulation is fully identical to the system), $A = A^{sim}$ i.e. $\rho_{TTR} = \rho_{LGS}$. In the *isoplanatic limit* (i.e. either LGS at infinite range in the direction of the science point of interest, or LGS at finite range coinciding with the science point of interest), $A = 1 = A^{sim}$ i.e. $\rho_{TTR} = \rho_{LGS}$. In these two limits, the TTR science SF reconstruction error is equal to the reconstruction error of the LGS SF. On the other hand, for the balanced filter, we have :

$$\rho_{TTR} = \frac{\rho_{LGS}}{\rho_{LGS}^{sim}} \frac{A}{A^{sim}}, \tag{2.14}$$

which clearly has the advantage to perfectly reconstruct the TTR SF in the matched simulation limit since both numerators and denominators cancel out in that limit i.e. $\rho_{TTR} = 1.$ In the isoplanatic limit, we have $\rho_{TTR} = \rho_{LGS} / \rho_{LGS}^{sim}$ for the balanced filter.

2.2. TT SF filter

The TT SF filter follows the same principles as the TTR SF filter, with the additional complexity that multiple low-order NGS WFSs are involved to perform tomographic reconstruction of a small number of low-order modes invisible to the TTR LGS WFSs. Typically, 5 NGS modes are reconstructed: global TT and 3 tilt anisoplanatism (TA) quadratic modes distributed on two atmospheric layers. The TT SF filter is defined as a ratio of system-to-simulation TT SFs for the science field point of interest. The unbalanced filter is therefore defined as:

$$W_{TT} = \frac{\hat{D}_{TT,NGS}}{D_{TT}^{sim}}, \tag{2.15}$$

where $\hat{D}_{TT,NGS}$ denotes the reconstructed residual TT SF, obtained from the reconstructed denoised tomographic NGS mode covariance matrix projected onto TT along the science direction. Mathematically, this covariance matrix can expressed as follows :

$$\hat{C}_{TT,NGS} = P_{TT} H_M R_{NGS} (C_{NGS,telem} - C_{NGS,nse}) R_{NGS}^T H_M^T P_{TT}^T, \quad (2.16)$$

where P_{TT} denotes aperture-plane projection onto TT, H_M propagates the reconstructed NGS atmospheric modes onto the aperture-plane along the science direction of interest, R_{NGS} is the NGS modal reconstructor, $C_{NGS,telem}$ the noisy closed loop NGS WFS measurement covariance matrix, and $C_{NGS,nse}$ the NGS WFS measurement noise covariance matrix. The same procedure has been described by Flicker [14] (in fact (2.16) is identical to (12) in [14]). Note that for the unbalanced filter, D_{TT}^{sim} cancels out in (2.15) and (2.9), i.e. the TT SF reconstruction error is given by:

$$\rho_{TT} = \rho_{TT,NGS}. \quad (2.17)$$

As for the TTR filters, the balanced TT filter is defined with the reconstructed (as opposed to actual) simulation TT SF as denominator, i.e.

$$W_{TT} = \frac{\hat{D}_{TT,NGS}}{\hat{D}_{TT,NGS}^{sim}}, \quad (2.18)$$

where both numerator and denominator are computed using (2.16), with the inner telemetry covariance matrix representing respectively system and simulation telemetry. The TT SF reconstruction error is then expressed as follows :

$$\rho_{TT} = \frac{\rho_{TT,NGS}}{\rho_{TT,NGS}^{sim}}, \quad (2.19)$$

which is unity (i.e. zero TT reconstruction error) in the matched simulation limit.

2.3. Figures of merit

Finally, we describe a few figures of merit of interest. For imaging observations, SR and EE can be computed from the OTF as follows:

$$SR = \frac{\int d^2u OTF(u)}{\int d^2u OTF_{DL}(u)}, \quad (2.20)$$

$$EE(\Omega) = \Omega^2 \int d^2u OTF(u) \mathrm{sinc}(u_x\Omega) \mathrm{sinc}(u_y\Omega), \quad (2.21)$$

where Ω denotes the angular width of the square integration domain. For astrometric studies, the angular separation between two PSFs can be computed from the location of the peak of their cross-correlation, which can be performed in Fourier space as follows:

$$d = \| \arg\max_\theta \int d^2u OTF_1(u) OTF_2^*(u) e^{-2i\pi u^T \theta} \|. \quad (2.22)$$

Each figure of merit can be evaluated for the 4 error sources described in this paper, namely (i) the long-exposure/stationarity assumption, (ii) the TT decoupling assumption, and finally (iii) the TTR and (iv) TT SF reconstruction errors. The various results of such a study carried out to support the design of NFIRAOS will be reported in a forthcoming publication.

3. Acknowledgements

The authors gratefully acknowledge the support of the TMT partner institutions. They are the Association of Canadian Universities for Research in Astronomy (ACURA), the California Institute of Technology and the University of California. This work was supported as well by the Gordon and Betty Moore Foundation, the Canada Foundation for Innovation, the Ontario Ministry of Research and Innovation, the National Research Council of Canada, and the U.S. National Science Foundation. L.Gilles's email address is lgilles@caltech.edu

4. References

1. P.B.Cameron, M.C.Britton and S.R.Kulkarni, ``Precision astrometry with adaptive optics,'' in ``Adaptive Optics Systems,'' N.N.Hubin, C.E.Max and P.L.Wizinowich, eds., Proc. Soc. Photo-Opt. Instrum. Eng. **7015**, 70150A-1 - 70150A-9 (2008).

2. P.B.Cameron, M.C.Britton and S.R.Kulkarni, ``Precision astrometry with adaptive optics,” Astron. J. **137**, 83-93 (2009).
3. C.Schödel, ``Accurate photometry with adaptive optics in the presence of anisoplanatic effects with sparsely sampled PSF: the Galactic center as an example of a challenging target for accurate AO photometry," Astron. Astrophys. **509**, A58 (2010).
4. R.Davies, H.Engel, E.Hicks, et. al.,``Dissecting Galaxies with Adaptive Optics," in ``Adaptive Optics Systems II," B.L.Ellerbroek, M.Hart, N.Hubin, P.L.wizinowich, eds., Proc. Soc. Photo-Opt. Instrum. Eng. **7736**, 7736G-1 - 7736G-9 (2010).
5. M.Ammons, E.Bendek and O.Guyon, ``Microarcsecond relative astrometry from the ground with a diffractive pupil,” Proc. Soc. Photo-Opt. Instrum. Eng. **8151**, 81510T (2011).
6. G.Herriot, D.Andersen, J.Atwood, et. al., ``NFIRAOS: TMT's facility adaptive optics system," in ``Adaptive Optics II," B.L.Ellerbroek, M.Hart, N.Hubin and P.L.Wizinowich, eds., Proc. Soc. Photo-Opt. Instrum. Eng. **7736**, 77360B-1 - 77360B-8 (2010).
7. B.Ellerbroek, S.Adkins, D.Andersen, et. al., "First light adaptive optics systems and components for the Thirty Meter Telescope", in ``Adaptive Optics Systems II," B.L.Ellerbroek, M.Hart, N.Hubin and P.L.Wizinowich, eds., Proc. Soc. Photo-Opt. Instrum. Eng. **7736**, 773604-1 - 773604-14 (2010).
8. J.P.Véran F.Rigaut, H.Maitre and D.Rouan, ``Estimation of the adaptive optics long-exposure point-spread function using control loop data," J. Opt. Soc. Am. A **14**, 3057-3069 (1997).
9. T.Fusco, J.-M.Conan, L.M.Mugnier, V.Michau and G.Rousset, ``Characterization of adaptive optics point spread function for anisoplanatic imaging. Application to stellar field deconvolution," Astron. Astrophys. Suppl. Ser. **142**, 149-156 (2000).
10. M.C.Britton,``The anisoplanatic point-spread function in adaptive optics," Pub. Astron. Soc. Pac. **118**, 885-900 (2006).
11. L.Jolissaint, C.Neyman, J.Christou, P.Wizinowich and L.Mugnier, “First successful adaptive optics PSF reconstruction at W.M.Keck observatory,” http://arxiv.org/abs/1202.3486 (2012).
12. R.Flicker,``PSF reconstruction for Keck AO," W.M.Keck Observatory, 65-1120 Mamalahoa Hwy., Kamuela, HI 96743, USA (unpublished). Available online at http://www.oir.caltech.edu/twiki_oir/bin/view/Keck/NGAO/PSF
13. A.Tokovinin, M.Le Louarn and M.Sarazin, ``Isoplanatism in a multiconjugate adaptive optics system," J. Opt. Soc. Am. A **17**, 1819-1827 (2000).
14. R.Flicker, F.Rigaut and B.Ellerbroek, ``Tilt anisoplanatism in laser guide star based multi conjugate adaptive optics. Reconstruction of the long exposure point spread function from control loop data”, Astron. Astrophys. **400**, 1199-1207 (2003).
15. L.Gilles and B.L.Ellerbroek, ``Real-time turbulence profiling with a pair of laser guide star Shack-Hartmann wavefront sensors for wide-field adaptive optics systems on large to extremely large telescopes”, J. Opt. Soc. Am. A **27**, A76-A83 (2010).
16. L.Wang and B.L.Ellerbroek, “Fast end-to-end multi-conjugate AO simulation using graphical processing units and the maos simulation code”, this conference (2012).
17. L.Gilles and B.L.Ellerbroek, “Long exposure adaptive optics point spread function sensitivity to cross-coupling between low- and high-order wavefront modes,” submitted to J. Opt. Soc. Am. A (2012).
18. B.Ellerbroek and F.Rigaut, “Methods for correcting tilt anisoplanatism in laser guide star based multiconjugate adaptive optics,” J. Opt. Soc. Am. A **18**, 2539-2547 (2001).
19. C.Correia, J.P.Verant, B.Ellerbroek, L.Gilles and L.Wang, “Laser-guide star point spread function reconstruction for extremely large telescopes,” this conference (2012).